Mandibular Forces During Simulated Tooth Clenching

Tom W.P. Korioth, BOd, Cir Dent, PhD
Assistant Professor
Department of Oral Science
Minnesota Dental Research Center for Biomaterials and Biomechanics
School of Dentistry
University of Minnesota
16-212 Moos Tower
515 Delaware Street SE
Minneapolis, Minnesota 55455

Alan G. Hannam, BDS, PhD, FDS, RCS
Professor
Department of Oral Biology
Faculty of Dentistry
The University of British Columbia
Vancouver, British Columbia
Canada

Correspondence to Dr Korioth

Differential, functional loading of the mandibular condyles has been suggested by several human morphologic studies and by animal strain experiments. To describe articular loading and the simultaneous forces on the dental arch, static bites on a three-dimensional finite element model of the human mandible were simulated. Five clenching tasks were modeled: in the intercuspal position; during left lateral group effort; during left lateral group effort with balancing contact; during incisal clenching; and during right molar clenching. The model's predictions confirmed that the human mandibular condyles are load-bearing, with greater force magnitudes being transmitted bilaterally during intercuspal and incisal clenching, as well as through the balancing-side articulation during unilateral biting. Differential condylar loading depended on the clenching task. Whereas higher forces were found on the lateral and lateroposterior regions of the condyles during intercuspal clenching, the model predicted higher loads on the medial condylar regions during incisal clenching. The inclusion of a balancing-side occlusal contact seemed to decrease the forces on the balancing-side condyle. Whereas the predicted occlusal reaction forces confirmed the lever action of the mandible, the simulated force gradients along the tooth row suggest a complex bending behavior of the jaw.

J OROFACIAL PAIN 1994;8:178–189.

Several investigators have commented upon the possibility of differential mechanical loading within the temporomandibular joint (TMJ).[1–4] The morphologic characteristics of the TMJ and the deformation in the subcondylar region of the mandibular ramus both suggest that the lateral thirds of the condyles may experience higher compressive forces during certain clenching tasks. Studies of apparently healthy human TMJs removed at autopsy have demonstrated zones of high-density cortical bone in the lateral region of the joint,[5] and increases in the size of the lateral facet of the condyles have been associated with increased tooth wear.[6] Examinations of diseased TMJs have suggested that deviations in form (DIFs) or osteoarthrosis (OA) may be caused by an increase in unfavorable biomechanical loading,[7] and that DIF and OA are usually located in the lateral and central aspects of the TMJ.[3,8] Deviations in form affect mainly the condyles, and OA is more frequent in the temporal components[9,10] or discs.[10] It is, however, important to note that these results are based on morphologic observations only, and that the biochemical pattern of OA might differ in location from the morphologic one.

Various animal experiments have shown that the mandible deforms in response to activation of the jaw muscles. The mammalian mandibular corpus can deform transversely, parasagittally, and in a rotational manner during function, and these patterns may

occur alone, in combination, unilaterally, or bilaterally.[4,11-17] In the monkey, jaw deformations have proven to be complex and are mainly characterized by vertical and rotational components. During unilateral biting, the macaque's jaw seems to deform around its long axis on the working side,[15] and the same effect has recently been observed in the simulated human mandible.[18] However, although differential loading at the condyles may result from rotational deformation of the rami, the rotational sense may vary according to the clenching task involved.[16] Thus, the distribution of forces on the condylar surfaces may differ between biting tasks due to differences in muscle activities. It is therefore possible that during some static activities, the lateral condylar thirds may not be more heavily loaded than other condylar areas.

To determine whether the condyle is differentially loaded during function, it is necessary to quantify these loads over the entire condylar surface. Although surface loads have been quantified three-dimensionally in other articulations (such as the glenohumeral joint) by means of stereophotogrammetry[19] and miniature piezoresistive transducers implanted superficially in the femoral head cartilage,[20] measurement of human condylar forces during jaw function remains elusive. Furthermore, the few experiments that have attempted to quantify these forces in animals did not adequately control jaw function or measure loads simultaneously from multiple surface points.[21,22]

The finite element (FE) modeling provides a way of resolving the many forces acting on the jaw while taking into account its shape and the rheological properties of its various components. In the present study, the hypothesis that the differential static loading of the human mandibular condyle differs between clenching tasks was tested. For this purpose, the distribution of loads on the upper condylar surfaces during simulated symmetric and asymmetric tooth-clenching tasks were quantified and compared. In addition, the magnitudes of tooth forces created simultaneously at multiple dental locations during these tasks were investigated.

Materials and Methods

Finite element modeling is an advanced numerical technique developed for engineering structural analysis. It solves a complex problem by redefining it as the summation of the solutions of a series of interrelated simpler problems. The first step is to subdivide the complex geometry into a suitable mesh of smaller elements. The finite elements are interconnected at specified points (nodes) on the element boundaries with defined degrees of freedom. Since the actual variation of the field variable (ie, displacement, stresses, or strains) inside the continuum of the structure is not known, it is assumed that the variation of the field variable within the specific finite element can be represented by a selected mathematical function. The use of functions allows generation of a series of equilibrium equations (one per nodal degree of freedom) that, when appropriately summed across the entire geometry and solved simultaneously, define the structure response of the system being considered. These equations are usually solved using matrix solution techniques. Once the nodal values of the field variables have been calculated, these selected functions are again used to solve for the field variable within each of the element regions.[23] Although several other modeling techniques, such as photoelasticity and holography, are available to quantify surface stresses on a structure, the FE technique was chosen because it is flexible enough to permit inclusion of the majority of pertinent variables affecting the masticatory system. These variables are, among others, the capability of allowing multiple muscular loads to act on any area of the model and in various directions, the selective action of multiple dental and articular restraints, and the possibility to apply realistic (ie, inhomogeneous and anisotropic) material properties to all structures in the model, in particular to the cortical bone.

To build a structural FE jaw model, the anatomy of the mandible had to be reconstructed in the computer and then divided into multiple finite elements interconnected at their corners. This process is described in detail elsewhere[18,24] and will be briefly explained in the following paragraphs.

A freshly dissected and fully dentate human mandible was imaged by means of computerized tomography (CT) (Siemens Somatom DR 2, Siemens, Munich, Germany). All dental and cortical bone outlines were traced sequentially on acetate overlays, digitized, and assembled into a three-dimensional (3-D) wire-frame model with available software (I-DEAS 6.0, SDRC, Milford, OH). Teeth were modeled with single or bifurcated roots, including their periodontal ligaments and laminae durae (Fig 1). The structure of the TMJs was modeled as a two-layered "cap," in which the first layer consisted of the combined thicknesses of condylar, articular, and temporal fibrocartilage, and the second consisted of temporal cortical bone.[25] This permitted analysis of the stress distribution on the condyles and allowed for

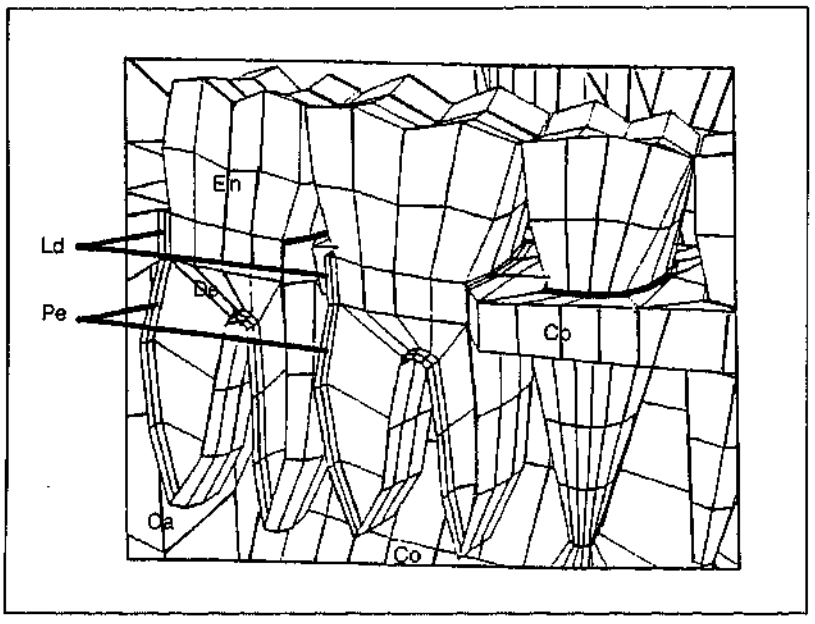

Fig 1 FE model of the dentate human mandible; cut window of the right corpus displays the underlying tissue components. Many cancellous bone elements were deleted to reveal the dental roots. (Co = cortical bone; Ca = cancellous bone; En = enamel; De = dentin; Ld = lamina dura; Pe = periodontal ligament.)

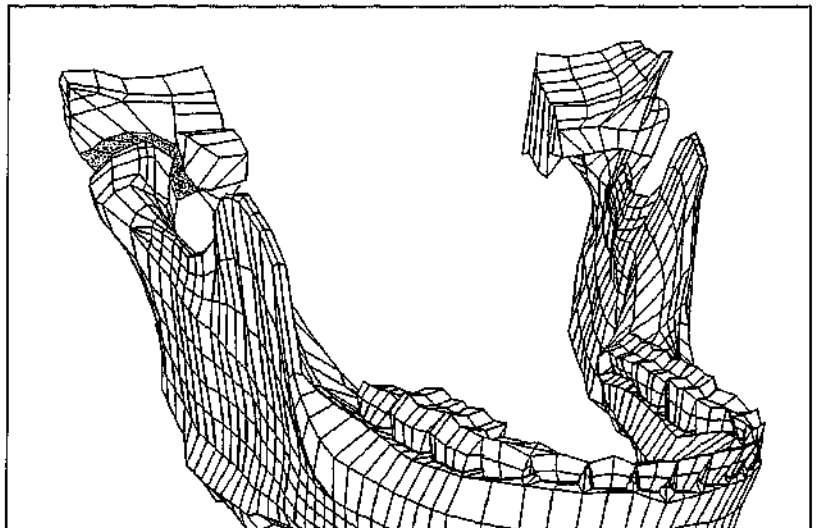

Fig 2 FE model of the human mandible showing hidden line view of the discretized element mesh seen anterolaterally from the right side. Dental and articular restraints, as well as the muscle loads, have been omitted for clarity. Some elements of the right TMJ have been deleted to show the presence of a fibrocartilaginous pad (stippled) between the condyle and the temporal bone.

the "buffering" effect of the articular disc against the rigid temporal bone. The fully assembled model consisted of 5,926 linear brick- and wedge-shaped elements with 7,375 nodes (Fig 2). Its different components were assigned material characteristics believed to conform to the best data available in the literature.[18] Prior to its use, the FE model was submitted to convergence and validation tests.[24]

The FE model was then used to simulate five static biting tasks: clenching in the intercuspal position (ICP), left lateral group effort (LGF), left lateral group effort with a cross-arch balancing contact on the second molar (LGF+B), incisal clenching (INC), and right unilateral molar clenching (RMOL). To simulate muscle forces over wide areas of attachment, the model was loaded with multiple force vectors. Groups of parallel vectors simulated nine pairs of masticatory muscles (superficial and deep masseter; anterior, middle, and pos-

terior temporalis; medial pterygoid; superior and inferior lateral pterygoid; and anterior digastric) assumed to be directly attached to bone (Fig 3). Their directions were derived algebraically as unit vectors (ie, direction cosines) from single vectors of muscular attachment available in the literature and summarized in Table 1. The magnitude of the total muscle force (M_{ir}) exerted by each muscle during isometric contraction was given by the product:

$$[X_{Mi} \cdot K] \cdot EMG_{Mi} = M_{ir}$$

where X_{Mi} is the cross-sectional area of muscle M_i in cm^2, K is a general conversion constant for skeletal muscle (expressed in N/cm^2), and EMG_{Mi} is the ratio or scaled value of the muscle contraction relative to its maximum possible activity for any task.[26,27] The product $[X_{Mi} \bullet K]$ is referred to as the Weighting Factor given to the muscle Mi, and the value EMG_{Mi} is referred to as its Scaling Factor (Table 2). The product of M_{ir} and its corresponding unit vector thus yielded the orthogonal vector force components, which were subsequently equally divided between the nodes comprising the corresponding area of muscle attachment (Table 2). In the case of nodes that included parts of two different muscles, the latter's respective force components were combined vectorially.

For occlusal tasks involving posterior teeth, the model was restrained only from vertical movement at the lateral and central thirds of the occlusal surfaces corresponding to supporting cusp and occlusal fossae contact zones. Eighty-four nodes during ICP, 44 nodes in LGF, 45 nodes during LGF+B, 42 nodes in INC, and 6 nodes in RMOL were vertically restrained during the corresponding clenching tasks. For those involving the anterior teeth, restraints were placed on the entire incisal surface of each tooth involved. These restraints acted only perpendicularly to the occlusal plane (y-direction) at the lower supporting cusps, thus allowing freedom of displacement anteroposteriorly and lateromedially in the horizontal plane. Restraints were also placed bilaterally at the endosteal cortical surfaces of the temporal bones. These simulated the fixation of the cranium and allowed free displacement of the jaw against the disclike structure.

The five clenches were simulated with both condyles centered in their glenoid fossae. All simulations were carried out with the I-DEAS package on a Hewlett-Packard 9000-series-380 UNIX-based minicomputer with a high-resolution workstation (HP 98789A) and peripherals (Palo Alto, CA).

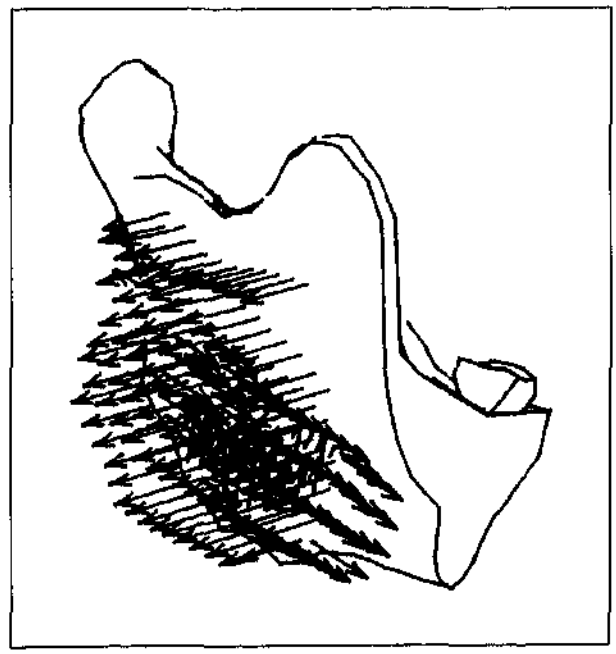

Fig 3 FE model of the human mandible showing right ramus with multiple parallel vectors simulating the masseter muscle loads. All vectors are graphically represented by their x, y, and z components and appear to be embedded in the model due to the nature of the display.

Results

Whereas the summed magnitudes of condylar forces were similar bilaterally during the symmetric clenching tasks (ICP and INC) (Table 3), forces tended to be higher on the upper lateral thirds of both condyles during ICP and bilaterally on the upper medial condylar thirds during INC (Fig 4). Although on average the condylar force magnitudes were quite similar during these tasks, higher maximums were predicted for INC on the medial condylar thirds than for ICP (Table 3).

During asymmetric clenching, different patterns of forces affected the balancing-side condyles. Whereas forces were highest on the upper lateral third for RMOL, they were highest on the upper medial thirds of the balancing-side condyles during LGF+B and LGF (Fig 4). On the working side condyles, areas of high force intensity were mainly located posterolaterally in both lateral group efforts (LGF and LGF+B) and anteromedially during RMOL (Fig 4).

In RMOL, the left balancing-side condyle experienced the highest average and total forces overall, and that on the working side showed smaller magnitudes (Table 3). Similar trends of force mag-

Table 1 Directions of Muscular Orthogonal Components Derived as Unit Vectors (ie, Direction Cosines) From Single Vectors of Muscular Attachment

	Right side			Left side		
Muscles	cos-x	cos-y	cos-z	cos-x	cos-y	cos-z
Superficial masseter	–0.207	0.884	0.419	0.207	0.884	0.419
Deep masseter	–0.546	0.758	–0.358	0.546	0.758	–0.358
Medial pterygoid	0.486	0.791	0.373	–0.486	0.791	0.373
Anterior temporalis	–0.149	0.988	0.044	0.149	0.988	0.044
Middle temporalis	–0.222	0.837	–0.500	0.222	0.837	–0.500
Posterior temporalis	–0.208	0.474	–0.855	0.208	0.474	–0.855
Inferior lateral pterygoid	0.630	–0.174	0.757	–0.630	–0.174	0.757
Superior lateral pterygoid	0.761	0.074	0.645	–0.761	0.074	0.645
Anterior digastric	–0.244	–0.237	–0.940	0.244	–0.237	–0.940

When seen from the front, the xz-plane was parallel to the floor, with the +x-axis oriented toward the right, the +y-axis running upward, and the +z-axis oriented forward (anteriorly).

Table 2 Node Number, Weighting, and Scaling Factors Assigned to the Masticatory Muscles for Five Clenching Tasks

	Node number		Weighting factor	Scaling factor									
				ICP		LGF		LGF + B		INC		RMOL	
Muscles	Right	Left	(Newton)	Right	Left	Right	Left	Right	Left	Right	Left	Right	Left
Superficial masseter	67	67	190.4	1.00	1.00	0.27	0.18	0.26	0.12	0.40	0.40	0.72	0.60
Deep masseter	38	38	81.6	1.00	1.00	0.26	0.36	0.26	0.36	0.26	0.26	0.72	0.60
Medial pterygoid	51	50	174.8	0.76	0.76	0.76	0.07	0.73	0.09	0.78	0.78	0.84	0.60
Anterior temporalis	43	40	158.0	0.98	0.98	0.07	0.66	0.23	0.54	0.08	0.08	0.73	0.58
Middle temporalis	18	18	95.6	0.96	0.96	0.06	0.64	0.12	0.57	0.06	0.06	0.66	0.67
Posterior temporalis	15	15	75.6	0.94	0.94	0.06	0.62	0.08	0.59	0.04	0.04	0.59	0.39
Inferior lateral pterygoid	5	5	66.9	0.27	0.27	0.14	0.59			0.71	0.71	0.30	0.65
Superior lateral pterygoid	4	4	28.7	0.59	0.59	0.08	0.20			0.50	0.50		
Anterior digastric	8	8	40.0	0.28	0.28	0.38	0.51			0.50	0.50		

Table 3 Force Magnitudes on the Top Condylar Surfaces During Various Clenching Tasks (Average, Maximum, and the Sum of Forces are Shown for 41 Nodes Located on Each Upper Right and Left Condylar Surface)

	Clenching tasks									
	ICP		LGF		LGF + B		INC		RMOL	
Condylar forces (Newtons)	Right	Left	Right	Left	Right	Left	Right	Left	Right	Left
Average	3.1	2.7	2.6	1.2	2.2	1.4	2.9	3.1	2.4	3.5
Maximum	7.2	7.4	7.2	3.6	6.4	3.8	9.0	10.2	7.5	9.5
Total	129	111	106	50	88	55	121	125	98	145

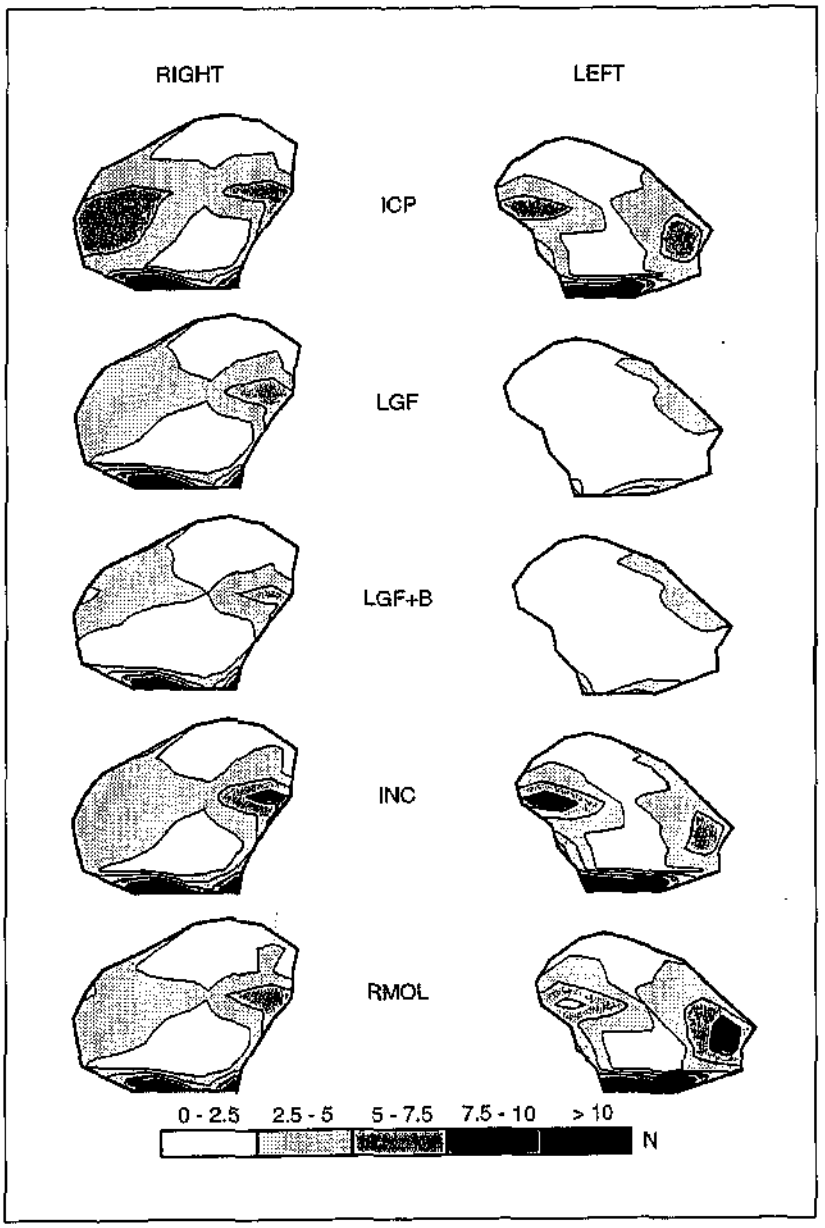

Fig 4 Distribution of predicted forces on the top condylar surfaces. The numbers on the plotted force-line contours reflect the specific levels of force magnitude.

nitudes were also observed during lateral group clenching efforts (LGF and LGF+B), where the right balancing-side condyle showed higher forces than the left working side. The balancing- to working-side ratio of forces was approximately 3:2 for both RMOL and LGF+B and 2:1 for LGF. These results agree with predictions from rigid static jaw models[28-31] and can be explained by a longer moment arm from the muscle resultant force to the balancing-side condyle than to the working-side condyle.

Figure 5 illustrates the distribution of occlusal reaction forces on the teeth chosen to restrain the jaw from moving. These reaction forces could be viewed as the bite forces elicited by the actions of the masticatory muscles. During ICP, occlusal forces were highest on the most posterior tooth locations and decreased anteriorly. They were least in the premolar region and rose again to form two distinct peaks at the canines. In LGF, the occlusal forces were relatively low in magnitude, with a peak at the left canine. During LGF+B, however, the tooth forces were highest at the most posterior locations on the working side and decreased progressively to reach the lowest value at the ipsilateral canine. Here, the balancing-side molar evidenced an occlusal force that was similar in magnitude to the highest value on the working side. In INC, the two lateral

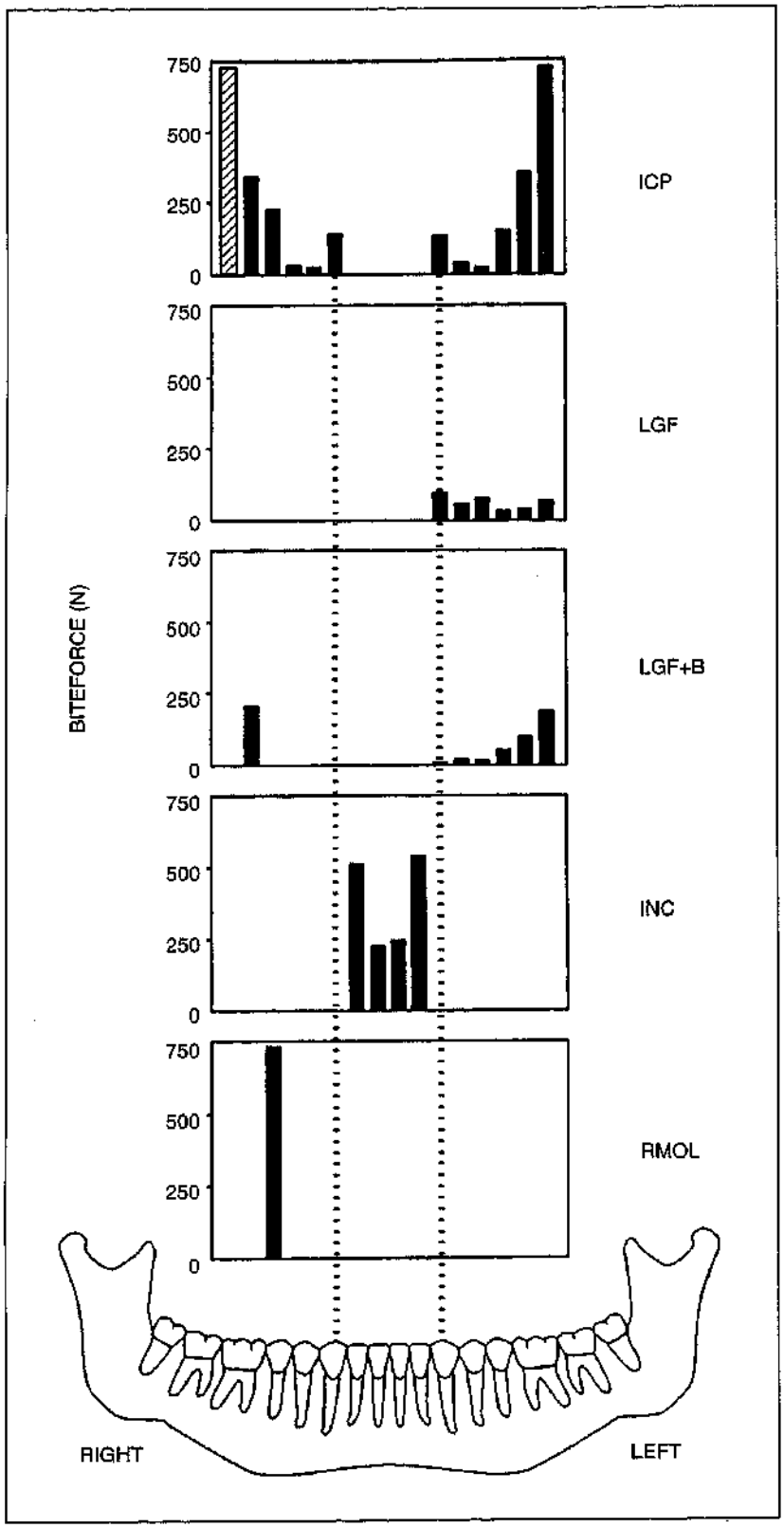

Fig 5 Occlusal reaction forces generated at the teeth during various clenching tasks. The teeth that were vertically restrained from movement were the canines to third molars bilaterally in intercuspal position (ICP, excluding the right third molar, which was not fully erupted and whose theoretical reaction force is shown in hatched form), the left canines to the last molars in left lateral group function (LGF), and the canines to the third molars on the left side plus the second molar on the right (balancing) side in left lateral group function plus balancing molar contact (LGF+B). In addition, the four incisors and the first right molar were not allowed to translate vertically during incisal clench (INC) and right unilateral molar clench (RMOL), respectively.

incisors experienced twice as much tooth force than did the two centrals. The highest bite force was produced during RMOL for all clenching tasks (731 N).

Discussion

Condylar Loads

The model's predictions confirmed the dependency of condylar load distribution on the type of clenching task. The simulations shown here support the notion that higher loads affect the lateral and lateroposterior regions of the condyles during specific clenching tasks. These localized loading patterns occurred during unilateral molar and bilateral intercuspal clenching. Whereas the former activity affected the contralateral (balancing) condyle, the latter activity affected both condyles due to its symmetry. During ICP, both condyles experienced higher loads at the poles and lower forces in their centers. Both condyles were deformed helically upward around their centers. While the lateral portion of each condyle was pushed upward and inward it also rotated posteriorly. In contrast, the medial poles were forced mainly upward and forward.

Incisal clenching loaded both condyles more anteromedially. This was probably due to the activity of the inferior lateral and medial pterygoid muscles bilaterally, which caused the two rami to be distorted medially and the corpora to be deformed parasagitally upward and forward.[32] During the two left lateral group effort clenches, the balancing-side condyles were loaded more anteromedially, which also most likely reflected the high medial deformation experienced by the balancing ramus due to the high degree of activity of the balancing medial pterygoid.

In bilaterally symmetric tasks, the force distribution patterns differed between sides. This was probably related to the slightly asymmetric muscle loading of the mandible, as well as the different bilateral shape of the condyles.[33] Whereas the right condyle had a round or oval frontal shape, the left one was flatter. The round shape seemed to distribute forces more evenly as evidenced by more consistent force patterns when compared with the flat shape, which tended to concentrate forces more at the edges of the surface. These results attest to the usefulness of the FE technique for modeling forces on irregular 3-D surfaces, as opposed to the use of other methods for which a relationship between condylar shape and loads can at best be inferred only indirectly.[34]

Mandibular condylar forces during jaw function have been measured in several in vivo animal experiments. Transducers have been attached to bony surfaces in the subcondylar region[35] or directly on top of the condyles.[21,22] Metallic prostheses have been implanted in the ramus near the joint,[36] and hydrostatic synovial fluid pressure has been analyzed within the superior aspect of the TMJ space.[37,38] All studies but one[22] have suggested that the TMJ is load-bearing, and that during unilateral mastication higher forces are transmitted through the balancing-side articulation than through the working-side articulation. Difficulties in determining the masticating or biting side may account for the data in the discrepant article, since this is a crucial step for the correct interpretation of the results. The ratio of bicondylar force distribution seems to be dependent on the bite point location. Our model's predictions also confirmed that the mandibular condyles are load-bearing, with the greatest forces being transmitted bilaterally through the TMJ during intercuspal and incisal clenching activities and through the balancing-side articulation during RMOL as well as LGF and LGF+B.

The site and number of occlusal contacts, and the direction of applied effort, influence activity in the jaw-closing muscles during tooth clenching.[39-45] Bilateral masseter muscle activity seems sensitive to differences in occlusal support between the left and right side of the dental arch.[46] In one study, the removal of six contacts on one side of a bite plane (leaving a single balancing-side molar contact) did not significantly change either the sidedness or the overall activity of the main jaw elevator muscles.[46] When the balancing contact was removed, however, muscle activity decreased by 21%. The authors suggested that in this case, the mandibular condyle on the balancing side may have taken much of the load previously taken by the balancing tooth contact. The predictions by the FE model confirmed the importance of a balancing-side molar contact in "stress-breaking" the balancing-side TMJ during clenching,[47] when the masseter and temporal muscles are bilaterally active in approximately equal amounts. If the muscle activities of the masseter and temporal muscles on the balancing side are increased during vertical clenching efforts on bite splints with an occlusal scheme such as group function with balancing-side molar contact,[48] then the articular loads on the balancing-side TMJ would increase slightly relative to the working side. These articular loads would probably still be less than those occurring when biting on splints with an occlusal scheme such as group

function but without a balancing-side molar contact, because the molar would transmit a high amount of the muscle force while simultaneously decreasing the loads at the condylar fulcrums. This notion is supported by the model's prediction of high occlusal reaction forces on the balancing-side second molar during LGF+B.

Tooth Forces

It is still very difficult to measure occlusal force three-dimensionally and simultaneously between several pairs of natural teeth, although some experiments have been performed on implant-supported prostheses.[49,50] The only simulated tasks that could be compared with in vivo data were RMOL and ICP. During RMOL, the predicted total reaction force of 731 N correlated quite well with averages measured by others (Ringquist,[51] 467 N; Helkimo et al,[52] 411 N; Mansour et al,[53] 774 N; Helkimo et al,[54] 471 N; Floystrand et al,[55] 500 N) and posterior bite forces predicted by two 3-D rigid computer models (Nelson,[56] 515 N; Koolstra et al,[57] 570 N [perpendicular to the occlusal plane]). It differed from that predicted by a third rigid static equilibrium model (Osborn et al,[58] 1029 N). This discrepancy may be due to differences in the muscle loads used in the latter study.

During intercuspal clenching, the highest occlusal forces were predicted for more posterior tooth locations. This compares favorably with published data[59] and can be explained biomechanically by the smaller tooth force moment arm and the more advantageous muscle to occlusal-force ratio. The most salient findings, however, were the bilateral peaks at the canines during ICP, at the lateral incisors during INC, and unilaterally at the canine during LGF. These force peaks occurred in the region that experienced not only parasagittal (lateral) bending the most due to its anterior location and hence long lever arm from the muscle load, but it was also a "turning point," where the rotational deformation of the corpora posteriorly was transformed into frontal and horizontal bending.[18] Thus, it is concluded that the higher occlusal reaction forces observed in the anterior region directly reflected the superimposition of bending and torsion of the corpus. Indirect evidence in support of this idea is given by the fact that the stiffest region along the mandibular corpus is at the lower border, inferior to the canine.[60,61] This region also seems to have the highest resistance to torsion.[62]

Although the model's predictions have demonstrated a good fit with experimentally derived strain data on a freshly excised mandible,[18,24] the model's simulations must be analyzed with caution. Among the most important variables that are still imperfectly modeled are the components of the TMJ, in particular the exclusion of synovial compartments and therefore, the omission of nonlinear frictional elements. In addition, the supposition that the disclike structure was centered in the glenoid fossa for all clenching tasks is obviously incorrect and may have had a significant impact on the distribution of condylar loads, especially for the incisal clenching task. These shortcomings were due to technical difficulties (ie, related to the software) and should be improved in the future.

Conclusion

The predictions of the FE model support the notion of differential loading at the mandibular condyles during selected tooth clenching tasks. The loading patterns are, however, task-dependent, and both the medial or the lateral condylar thirds can be heavily loaded. The lateral third of the upper condylar surface is more heavily loaded bilaterally during intercuspal clenching and unilaterally on the balancing side for a molar clench. The condylar surface is more heavily loaded anteromedially during incisal clenching due to the inward, upward, and forward deformation of the mandibular corpus. The inclusion of a molar contact on the balancing side might be advantageous in cases where bilateral articular force reduction is sought. The predicted occlusal reaction forces seem to reflect the bending characteristics of the jaw imposed by muscle action and the inherent elastic behavior of the mandibular tissues. Whereas the predicted occlusal reaction forces confirmed the lever action of the mandible, the simulated force gradients along the tooth row suggest a complex bending behavior of the jaw. Finite element modeling, provided it is carried out with care, seems to provide a powerful and sophisticated theoretical approach to use in future studies of jaw form and function. The approach, however, is still limited by the oversimplification of many structural components, the availability and reliability of suitable values for the many variables involved, and in the present case, conditions of static loading.

Acknowledgments

The authors gratefully acknowledge the help of Joy D. Scott in the computational aspects of this project.

References

1. Mofett BC, Johnson LC, McCabe JB, Askew HC. Articular remodelling in the adult human temporomandibular joint. Am J Anat 1964;115:119–142.
2. Molitor J. Untersuchungen über die Beanspruchung des Kiefergelenks. Z Anat Entwickl-Gesch 1969;128:109–140.
3. Öberg T, Carlsson GE, Fajers C-M. The temporomandibular joint: A morphologic study on a human autopsy material. Acta Odontol Scand 1971;29:349–383.
4. Hylander WL, Bays R. An in vivo strain-gauge analysis of the squamosal-dentary joint reaction force during mastication and incisal biting in Macaca mulatta and Macaca fascicularis. Archs Oral Biol 1979;24:689–697.
5. Werner JA, Tillman B, Schleicher A. Functional anatomy of the temporomandibular joint. Anat Embryol 1991;183:89–95.
6. Owen CP, Wilding RJC, Morris AG. Changes in mandibular condyle morphology related to tooth wear in a prehistoric human population. Archs Oral Biol 1991;36:799–804.
7. Åkerman S, Rohlin M, Koop S. Bilateral degenerative changes and deviation in form of temporomandibular joints. Acta Odontol Scand 1984;42:205–214.
8. Nannmark U, Sennerby L, Haraldson T. Macroscopic, microscopic and radiologic assessment of the condylar part of the TMJ in elderly subjects. An autopsy study. Swed Dent J 1990;14:163–169.
9. Richards LC. Tooth wear and temporomandibular joint change in Australian aboriginal populations. Am J Phys Anthropol 1990;82:377–384.
10. Holmlund A, Hellsing G, Axelsson S. The temporomandibular joint: A comparison of clinical and arthroscopic findings. J Prosthet Dent 1989;62:61–65.
11. Kakudo Y, Ishida A, Yoshimoto S. Strains in dog's jaw bones following implant insertion and a photoelastic study of implants and the jaw bones. J Osaka Dent Univ 1973;7:31–42.
12. Weijs WA, De Jongh HJ. Strain in mandibular alveolar bone during mastication in the rabbit. Archs Oral Biol 1977;22:667–675.
13. Hylander WL, Crompton AW. Jaw movements and patterns of mandibular bone strain during mastication in the monkey Macaca fascicularis. Archs Oral Biol 1986;31:841–848.
14. Hylander WL, Johnson KR, Crompton AW. Loading patterns and jaw movements during mastication in Macaca fascicularis: a bone-strain, electromyographic, and cineradiographic analysis. Am J Phys Anthropol 1987;72: 287–314.
15. Hylander WL. The functional significance of primate mandibular form. J Morphol 1979;160:223–240.
16. Hylander WL. In vivo bone strain in the mandible of Galago crassicaudatus. Am J Phys Anthropol 1977;46:309–326.
17. Hylander WL. Mandibular function in Galago crassicaudatus and Macaca fascicularis: An in vivo approach to stress analysis of the mandible. J Morphol 1979;159: 253–296.
18. Korioth TWP. Finite Element Modelling of Human Mandibular Biomechanics [Thesis]. Vancouver: The University of British Columbia, 1992.
19. Soslowsky W, Flatow EL, Bigliani LU, Pawluk RJ, Ateshian GA, Mow VC. Quantitation of in situ contact areas at the glenohumeral joint: A biomechanical study. J Orthop Res 1992;10:524–534.
20. Brown TD, Shaw DT. In vitro contact stress distributions in the natural human hip. J Biomechanics 1983;16: 373–384.
21. Brehnan K, Boyd RL, Laskin J, Gibbs C, Mahan P. Direct measurement of loads at the temporomandibular joint in Macaca arctoides. J Dent Res 1981;60:1820–1824.
22. Boyd RL, Gibbs C, Mahan PE, Richmond AR, Laskin JL. Temporomandibular joint forces measured at the condyle of Macaca arctoides. Am J Orthod Dentofac Orthop 1990;97:472–479.
23. Rao SS. The Finite Element Method in Engineering. New York: Pergamon Press, 1982.
24. Korioth TWP, Dechow PC, Hannam AG. 3-D finite element modeling and validation of a dentate human mandible [abstract]. J Dent Res 1992;71:781.
25. Hansson T, Öberg T, Carlsson GE, Kopp S. Thickness of the soft tissue layers and the articular disk of the temporomandibular joint. Acta Odontol Scand 1977;35:77–83.
26. Pruim GJ, de Jongh HJ, Ten Bosch JJ. Forces acting on the mandible during bilateral static bite at different bite force levels. J Biomechanics 1980;13:755–763.
27. Weijs WA, Hillen B. Relationship between the physiological cross-section of the human jaw muscles and their cross-sectional area in computer tomographs. Acta Anat 1984;118:129–138.
28. Gysi A. Studies on the leverage problem of the mandible. Dent Digest 1921 ;27:74,144,203–284,150,208.
29. Motsch A. Kaufunktion und Kiefergelenkbeanspruchung. Dtsch Zahnärztl Z 1968;23:819–835.
30. Hylander WL. The human mandible: Lever or link? Am J Phys Anthropol 1975;43:227–242.
31. Smith RJ. Mandibular biomechanics and temporomandibular joint function in primates. Am J Phys Anthropol 1978;49:341–350.
32. Korioth TWP, Hannam AG. Deformation of the human mandible during simulated tooth clenching. J Dent Res 1994;73:56–66.
33. Maeda Y, Korioth TWP, Wood WW. Stress distribution on simulated mandibular condyles of various shapes [abstract]. J Dent Res 1990;69.
34. Osborn JW, Baragar FA. Predicted and observed shapes of human mandibular condyles. J Biomechanics 1992;25:967–974.
35. Hylander WL. An experimental analysis of temporomandibular joint reaction force in macaques. Am J Phys Anthropol 1979;51:433–456.
36. Hohl TH, Tucek WH. Measurement of condylar loading forces by instrumented prosthesis in the baboon. J Maxillofac Surg 1982;10:1–7.
37. Roth TE, Goldeberg JS, Behrents RG. Synovial fluid pressure determination in the temporomandibular joint. Oral Surg 1984;57:583–588.
38. Ward DM, Behrents RG, Goldberg JS. Temporomandibular synovial fluid pressure response to altered mandibular positions. Am J Dentofac Orthop 1990; 98:22–28.
39. Williamson EH, Lundquist DO. Anterior guidance: Its effect on electromyographic activity of the temporal and masseter muscles. J Prosthet Dent 1983;49:816–823.
40. Shupe RJ, Mohamed SE, Christensen LV, Finger IM, Weinberg R. Effects of occlusal guidance on jaw muscle activity. J Prosthet Dent 1984;51:811–818.
41. MacDonald JWC, Hannam AG. Relationship between occlusal contacts and jaw-closing muscle activity during tooth clenching: Part I. J Prosthet Dent 1984;52:718–729.

42. MacDonald JWC, Hannam AG. Relationship between occlusal contacts and jaw-closing muscle activity during tooth clenching: Part II. J Prosthet Dent 1984;52: 862–867.
43. Manns A, Chan C, Miralles R. Influence of group function and canine guidance on electromyographic activity of elevator muscles. J Prosthet Dent 1987;57:494–501.
44. Belser UC, Hannam AG. The influence of altered working-side occlusal guidance on masticatory muscles and related jaw movement. J Prosthet Dent 1985;53:406–413.
45. Freesmeyer WB, Hüls A, Lutz R, Vogel J. Änderung der elektromyographisch aufgezeichneten Aktivität der Elevatoren durch experimentelle Okklusions- und Artikulationsstörungen. Dtsch Zahnärztl Z 1987;42: 374–379.
46. Wood WW, Tobias DL. EMG response to alteration of tooth contacts on occlusal splints during maximal clenching. J Prosthet Dent 1984;51:394–396.
47. Minagi S, Watanabe H, Sato T, Tsuru H. Relationship between balancing-side occlusal contact patterns and temporomandibular joint sounds in humans: proposition of the concept of balancing-side protection. J Craniomandib Disord Facial Oral Pain 1990;4:251–256.
48. MacDonald JWC. Occlusal contacts and jaw muscle activity in parafunctional clenching [Thesis]. Vancouver: The University of British Columbia, 1982.
49. Falk H. On occlusal forces in dentitions with implant-supported fixed cantilever prostheses. Swed Dent J 1990;69(suppl):1–40.
50. Merickse-Stern R, Geering AH, Bürgin WB, Graf H. Three-dimensional force measurements on mandibular implants supporting overdentures. Int J Oral Maxillofac Implants 1992;7:185–194.
51. Ringquist M. Isometric bite force and its relationships to dimensions of the facial skeleton. Acta Odontol Scand 1973;31:35–42.
52. Helkimo E, Carlsson GE, Carmeli Y. Bite force in patients with functional disturbances of the masticatory system. J Oral Rehabil 1975;2:397–406.
53. Mansour RM, Reynik RJ. In vivo occlusal forces and moments: I. Forces measured in terminal hinge position and associated moments. J Dent Res 1975;54:114–120.
54. Helkimo E, Ingervall B. Bite force and functional state of the masticatory system in young men. Swed Dent J 1978;2:167–175.
55. Fløystrand F, Kleven E, Oilo G. A novel miniature bite force recorder and its clinical application. Acta Odontol Scand 1982;40:209–214.
56. Nelson GJ. Three dimensional computer modelling of human mandibular biomechanics [Thesis]. Vancouver: The University of British Columbia, 1986.
57. Koolstra JH, van Eijden TM, Weijs WA, Naeije M. A three-dimensional mathematical model of the human masticatory system predicting maximum possible bite forces. J Biomechanics 1988;21:563–576.
58. Osborn JW, Baragar FA. Predicted pattern of human muscle activity during clenching derived from a computer assisted model: symmetric vertical bite forces. J Biomechanics 1985;18:599–612.
59. Lundgren D, Falk H, Laurell L. Influence of number and distribution of occlusal cantilever contacts on closing and chewing forces in dentitions with implant-supported fixed prostheses occluding with complete dentures. Int J Oral Maxillofac Implants 1989;4:277–283.
60. Dechow PC, Schwartz-Dabney CL, Ashman RB. Elastic properties of the human mandibular corpus. In: Goldstein SA, Carlson DS (eds). Bone Biodynamics in Orthodontic and Orthopaedic Treatment. Ann Arbor, Michigan: Craniofacial Growth Series, Vol 27. Center for Human Growth and Development, The University of Michigan, 1992.
61. Dechow PC, Nail GA, Schwartz-Dabney CL, Ashman RB. Elastic properties of human supraorbital and mandibular bone. Am J Phys Anthropol 1993;90:291–306.
62. Demes B, Preuschoft H, Wolff JEA. Stress-strength relationships in the mandibles of hominoids. In: Chivers DJ, Wood BA, Bilsborough A (eds). Food Acquisition and Processing in Primates. New York: Plenum Press, 1984.